Metallic work function measurement in the range 2–3.3 eV using a blue light-emitting diode source

Reto Schletti,[a] Peter Wurz, and Theo Fröhlich
Physikalisches Institut, University of Bern, 3012 Bern, Switzerland

(Received 28 May 1998; accepted for publication 9 November 1999)

A new photoelectric method to monitor the work function of contaminated metallic surfaces in the range 2–3.3 eV using blue light-emitting diodes (LEDs) is presented. This method was specifically developed for an application onboard a spacecraft, where the simplicity of a system is a great asset. This technique makes it possible to follow the work function of a calibrated surface LED combination with a reproducibility of $\sim 2\%$ with only one blue LED and a device to count photoelectrons. The surface described in this paper is Cs/W(110). The work function changes with time due to adsorption of residual gas in the moderate vacuum environment (in the mid 10^{-8} mbar range). Determination of the work function with a standard photoelectric technique is used to calibrate the system. We then derive calibration curves for this specific surface LED combination which reduce the workfunction measurement to a simple current measurement. © *2000 American Institute of Physics.* [S0034-6748(00)04402-6]

I. INTRODUCTION

The low energy neutral atom (LENA) instrument[1,2]—an imaging mass spectrograph for low energetic neutral atoms on the IMAGE satellite mission[3]—is designed for remote sensing of magnetospheric plasma populations. Surface ionization was found to be the only ionization method meeting the boundary conditions imposed by the satellite (weight, space, and power among others) yielding sufficient ionization rates for the expected low fluxes in the energy range of 10 eV to 1 keV. The applicability of surface ionization in space instrumentation has been shown for Cs or Ba coated W(110).[1,4,5] Thereby, neutral atoms are scattered from a low work function (WF) surface and a significant fraction of the reflected particles become negative ions. These ions are then accessible for mass, energy, and direction analysis by established mass spectrometers in space plasma research.

Low-WF surfaces are typically generated by coating a metal surface with a thin layer of an electropositive metal. The states of the valence electron of the adsorbed atoms is partially depopulated (lying approximatively on the same level as the valence band of the metal). This causes an additional surface dipole layer, which reduces the WF markedly.[6] An extensively studied combination is Cs/W(110), used either with 0.6 monolayer or a full monolayer of Cs.[7–9] The WF shows a minimum of 1.45 eV for the submonolayer coverage and equals the value of bulk Cs (2.15 eV) for the full monolayer, which is far below the WF of bare W(110) substrate of 5.25 eV. The same mechanism works for barium which has a bulk WF of 2.5 eV.

Due to adsorption of electronegative residual gas atoms such as oxygen or hydrogen a new dipole layer of opposite sign starts to grow (this time the affinity level of the adsorbed atoms is partially populated) and the WF increases again. This increase of the WF with time reduces the negative ion fraction in the reflected beam. The time scale of the degradation of the converter surface depends on the residual gas density and composition. In earlier work[4,5] we found a close correlation of the WF and the ionization efficiency. The range of the WF useful for the application in the LENA instrument spans from 2 eV to more than 3 eV. In-fight calibration, i.e., the knowledge of the ionization efficiency of the surface at the time of data taking in space, is necessary for data evaluation and is only possible with a precise knowledge of the WF. After some time, typically one day[1,4] for the conditions expected on a space experiment, reconditioning of the surface (thermal cleaning and application of a new Cs layer) is necessary. The moment for performing this procedure will be chosen based on the WF data. Established laboratory techniques for the WF measurement turned out to be too complicated to be implemented for an application onboard a spacecraft. In this paper we present a new method to measure the WF of a surface in the range from 2 to 3.3 eV using blue light emitting diodes (LED).

II. THEORY

The measurement of the WF is based upon the photoeffect. If the energy $h\nu$ of a photon absorbed by a surface exceeds the WF Φ, an electron can be released. The electron gas in a potential well at $T=0$ K is filled up to the Fermi level (E_F), which lies below the vacuum level by the WF (see Fig. 1). The number of electrons released per quantum of light is[10]

$$N(h\nu) \propto \begin{cases} \dfrac{(h\nu-\Phi)^2}{(V_0-h\nu)^{1/2}} & (h\nu>\Phi) \\ 0 & (h\nu<\Phi) \end{cases}, \tag{1}$$

where V_0 stands for the vacuum potential. The collected photocurrent for monochromatic irradiation ($h\nu$ in the vicinity

[a]Electronic mail: schletti@phim.unibe.ch

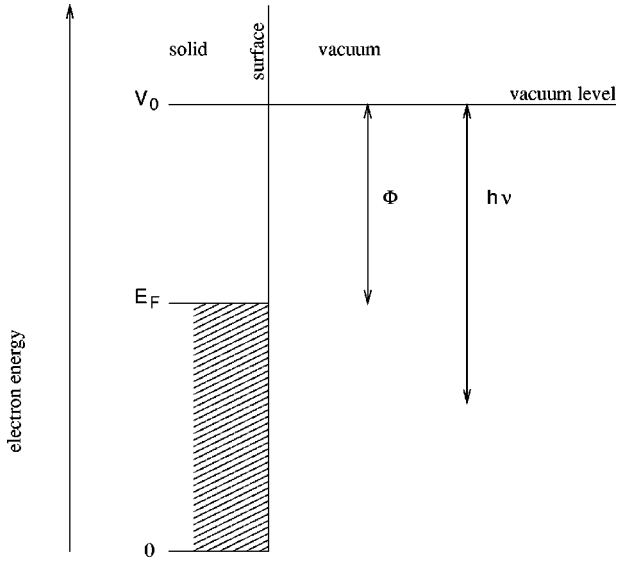

FIG. 1. Electron energy level diagram for a metal. The WF Φ is defined as the energy difference between the vacuum level V_0 and the Fermi level E_F. An electron from the conduction band (dashed area) can leave the surface only if the energy gained from a photon $h\nu$ is at least Φ.

of Φ) is then approximately proportional to the square of the energy difference of the photon and the WF, because the denominator $(V_0-h\nu)^{1/2}$ is varying slowly. Thus it is possible to measure the WF with a monochromatic light source of variable wavelength by scanning the photon energy and counting the photoelectrons. The WF is then equivalent to the energy of the photons at the onset of the release of photoelectrons. This is one of the established ways to determine the photoelectric WF and also the method used in our laboratory experiment. The schematics of this measurement are shown in Fig. 2.

If the light source is polychromatic the photocurrent $I(\Phi)$ is the integral of Eq. (1) multiplied with the spectrum $f(h\nu)$ of the light source

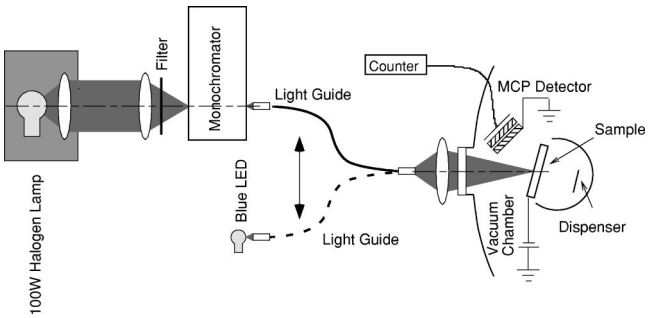

FIG. 2. Schematic of the experimental setup. The monochromatic light source of variable wavelength is formed with a 100 W QTH halogen lamp and a grating monochromator. The light is coupled into a fiber bundle and focused through a viewport onto the sample surface in the vacuum chamber. The emitted photoelectrons are accelerated by a weak electric field toward the MCP-detector capable of counting single electrons. The filter is used to block short wavelengths (below 400 nm) from entering the monochromator so that the second order diffraction peak does not interfere with the WF measurement. The fiber bundle can quickly be pulled off the monochromator and fixed in front of the LED and vice versa during the measurement of the calibration curves. The optical path remains the same for both measurements.

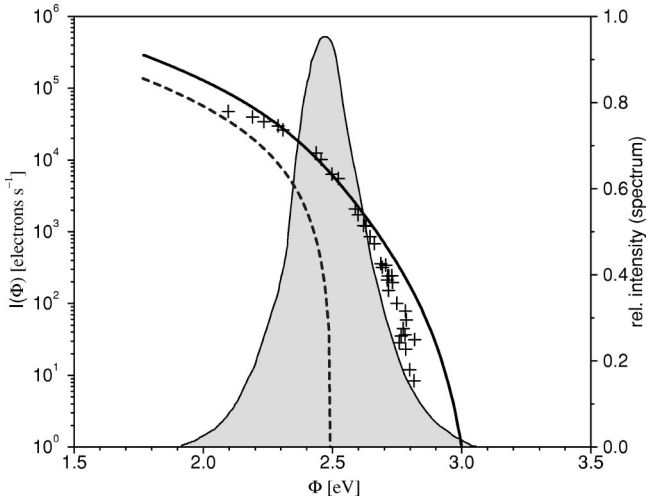

FIG. 3. Theoretical calibration curve $I(\Phi)$ for the GaN LED model R5B01-ML375 (solid line) and for a theoretical monochromatic light source with $h\nu=2.5$ eV (dashed line) calculated from Eq. (2). The measured calibration curve (plus symbols) is shown for comparison. The spectrum of the LED is also shown (filled area).

$$I(\Phi)=I_0\int_{\Phi}^{\infty}\frac{(h\nu-\Phi)^2}{(V_0-h\nu)^{1/2}}f(h\nu)h\,d\nu, \tag{2}$$

with I_0 being a constant depending on the intensity of the light source, on the index of reflection, and on the electron density of the surface (which defines the Fermi level). The photocurrent is now a function of the WF and of the spectrum $f(h\nu)$ of the light source (not of the mean photon energy only).

If the surface is irradiated with a constant light source like a LED, the amount of released photoelectrons $I(\Phi)$ is a measure of the WF only. If the WF now changes with time due to adsorption of atoms, the photocurrent will change with Φ being the main varying factor in Eq. (2). This can be used to monitor the WF of a surface once a calibration of the current function $I(\Phi)$ for that surface and light source has been established. The WF is then simply obtained by inversion of the current function $I(\Phi)\rightarrow\Phi(I)$. The measurement of the WF is consequently reduced to the measurement of an electric current. The schematics of this measurement are shown in Fig. 2.

In Fig. 3 we show an example of the calculated current function $I(\Phi)$ for a constant monochromatic light source with $h\nu=2.5$ eV and for the first LED tested in this paper (see Sec. III). The light spectrum of the LED $f(h\nu)$ is also shown in the same plot. One can see that the photocurrent strongly depends on the WF of the surface and covers several orders of magnitude. The WF can be followed up to the highest photon energies in the spectrum (the blue end), where the photocurrent decreases dramatically. In our application, the WF has to be followed as far up as possible, thus LEDs with short wavelength components in the blue or even in the UV spectral range are the preferred choice.

III. EXPERIMENTAL SETUP

An experiment to study surface ionization was built to investigate the suitability of various conversion surfaces for

their application on a space platform.[5,11] After baking out the system a residual gas pressure in the mid 10^{-8} mbar range typically is obtained. The residual gas composition is mainly H_2O and some air from tiny leaks. The charge state of an ion beam after reflection from a converter surface can be measured with a retarding potential analyzer (RPA) followed by an imaging microchannel plate (MCP). The angular scattering of the reflected beam can be measured with the same apparatus. The surface can be regenerated by thermal cleaning up to 1800 K and the subsequent application of a thin layer of Cs (or Ba) from a dispenser (SAES Getters), which yields surfaces with very low WF. It takes 45 s to deposit one monolayer of Cs based on manufacturer's specifications and our own measurements.[12] The surface is rotated toward the dispenser into a closed housing with a separate pumping port to avoid Cs contamination of the MCP during reconditioning (see Fig. 2). The variable monochromatic light source is obtained using a 100 W *quartz tungsten halogen* (QTH) lamp and a McPherson GM 252 1/4 m grating monochromator (range 350–800 nm). The light is then coupled into a high-grade fused silica fiber bundle (Oriel: 250–1200 nm) and focused (Oriel lens: 340–1500 nm) through a Balzers KODIAL glass viewport (350–2500 nm) onto the surface under investigation in the vacuum chamber. The spot size on the surface is about 2 mm in diameter. The fiber bundle can quickly be pulled off the monochromator and fixed in front of the LED and vice versa. Scattered and stray light can easily disturb the WF measurement, therefore, the light path from the source to the vacuum chamber is shielded from ambient light. All filaments inside the vacuum chamber are turned off during measurements to avoid stray light and stray electrons. A highpass filter (Oriel: 415–2750 nm) is used to block short wavelengths from entering the monochromator so that the second order diffraction peak does not interfere with the WF measurement (only used if the WF is lower than 3 eV). The photoelectrons are accelerated away from the surface (biased to $-200\,\mathrm{V}$) by a weak electric field ($E \sim 2\,\mathrm{kV\,m^{-1}}$) and detected with the position sensitive MCP detector capable of detecting single electrons.

The first LED we investigated was a blue GaN LED model R5B01-ML375 (Toyota Gosei) with a maximum intensity at $\lambda = 482\,\mathrm{nm}$, a spectral width [fullwidth at half maximum (FWHM)] of 65 nm, and a total luminosity of 50 mcd. The highest photon energy is approximately 3 eV. The spectrum is shown in Fig. 3. In our experiment we used a forward current of 10 mA to drive the LED and the power consumption was 150 mW.

The second LED was a Zn-doped InGaN/AlGaN LED model NLPB500 (Nichia Chemical Industries) with a peak wavelength of $\lambda = 450\,\mathrm{nm}$ and a spectral width (FWHM) of 70 nm, and a total luminosity of 2 cd. This diode has the property that the peak wavelength is shifted toward shorter wavelengths for increasing forward current.[13] In pulsed operation with a peak current of 2 A, instead of nominal 30 mA for direct-current (dc) operation, the light peak at 450 nm even saturates and an additional ultraviolet (UV) peak at 380 nm emerges.[14] In this mode the diode has to be driven with very short pulses to avoid damage. The driving circuit was taken from Ref. 14, where the LED is driven by an avalanche transistor (Zetex ZTX-415) at a repetition rate of 10 kHz. The achieved pulse length is 3 ns. We tested the LED in both, the dc mode and the alternating-current (ac) mode. In dc mode the power consumption was 100 mW. In pulsed mode the LED illuminates the surface only 0.003% of the time, resulting in a lower mean illumination than in dc mode and a mean power consumption of the circuit of 1 W.

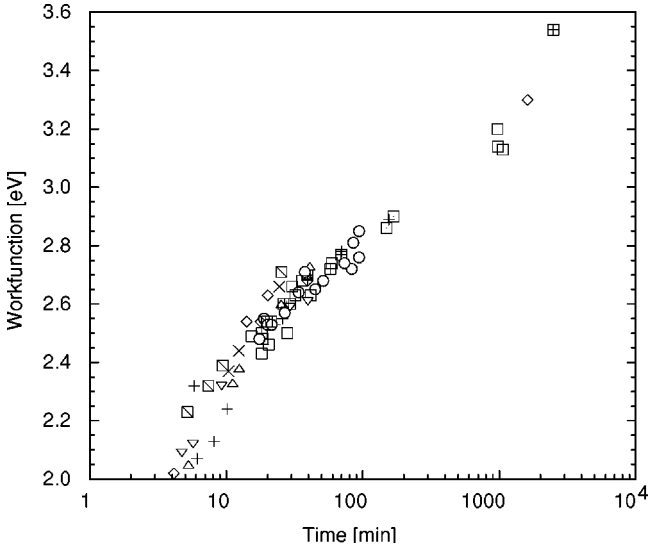

FIG. 4. Temporal evolution of the WF of the Cs/W(110) surface in our experiment. The increase of the WF with time, measured with the monochromator, is due to adsorption of residual gases. The different symbols indicate different runs, i.e., measurement series after cleaning of the surface and application of a new Cs layer.

IV. MEASUREMENTS

A measurement cycle was started with preparation of the surface to obtain a low WF by applying approximately one monolayer of Cs. The WF was then measured using the monochromator where the onset of the photoelectron emission when scanning down the wavelength was taken as the WF of the surface (see Sec. II). We can reproduce the onset wavelength to $\pm 5\,\mathrm{nm}$.[4] The uncertainty of the wavelength calibration of the monochromator has to be taken into account for absolute WF measurement. This systematic error introduced by the monochromator is however not important for our application since the ionization efficiency of the surface is calibrated with the same device (see Sec. I). In the first minutes after applying a fresh Cs layer the WF of the surface raises rapidly due to residual gas exposition (Fig. 4). The error for the first points is larger due to change of the WF during the measurement (~ 1 min). The progression of the WF is slightly different for two subsequent series due to different conditions between two series (e.g., Cs coverage, residual gas composition, and pressure). To interpolate the WF values for any time, a polynomial fit of second order in a semilogarithmic representation has been performed for each series, following

$$\Phi(t) = A_0 + A_1 \ln t + A_2 \ln^2 t. \tag{3}$$

Parallel to the WF measurement, the photo current $I(t)$ induced by the LED illumination of the surface is measured.

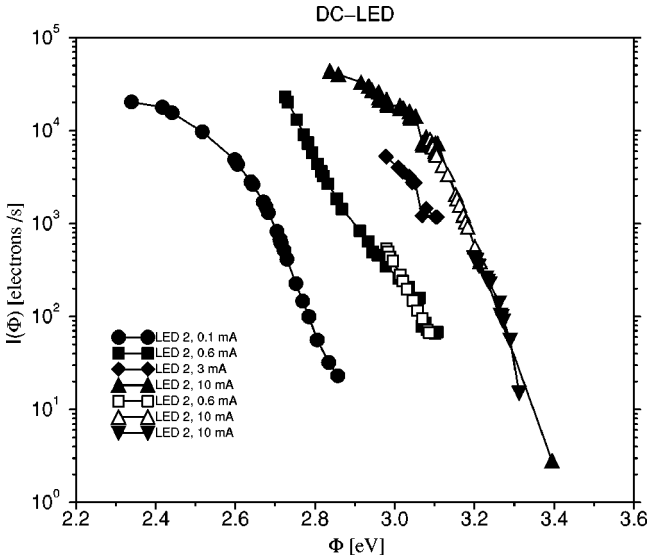

FIG. 5. The measured calibration curves $I(\Phi)$ in dc mode for the InGaN/AlGaN LED in our specific setup. In the first measurement series four forward currents were used: 0.1 (black circles), 0.6 (black squares), 1 (black diamonds), and 10 mA (black triangles). In the second series two currents were used: 0.6 (open squares) and 10 mA (open triangles). In the third series, the surface was heated only moderately to clean it from adsorbated residual gas but leaving a submonolayer of Cs on the surface. These data are represented by downward black triangles.

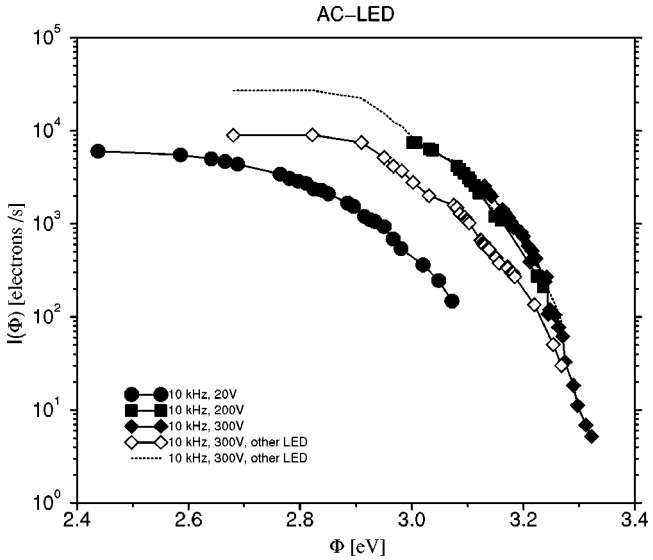

FIG. 6. The measured calibration curves $I(\Phi)$ for the InGaN/AlGaN LED operated in pulsed mode for three bias voltages (full symbols). An additional measurement with a second LED of the same type is also displayed (open symbols) and scaled for comparison with earlier measurements (dashed line). See the text for details.

For this purpose, the optics has to be switched after every data point (see Fig. 2). While the WF increases with time, the photocurrent decreases monotonically. From Eq. (3) we find the appropriate WF for the time t of the measured photocurrent $I(t)$. This leads to the current function

$$I(\Phi)=I[t(\Phi)]. \tag{4}$$

For one measurement series with the first LED the calibration curve $I(\Phi)$ is shown in Fig. 3 together with the theoretical curve calculated from the LEDs spectrum. The theoretical curve is scaled to fit the data points [I_0 from Eq. (2) is not calculable]. Differences between the theoretical $I(\Phi)$ curve and the measured data are attributed to saturation of the measurement electronics for small WF (high count rates), and to the simplicity of the assumptions in Eq. (2) for high WF. The assumption that I_0 remains constant during degradation of the surface (adsorption of residual gas atoms) is certainly not valid however the theory is only given to provide qualitative understanding of the phenomenon. For medium count rates there is a good agreement. At low count rates the statistical uncertainty increases due to the weak emission of the LED at short wavelengths. The background of the MCP detector (of the order of 10–100 counts/s) was measured and subtracted which also increases the error. Nevertheless the obtained calibration curve is monotonic and can be inverted. The WF can be monitored up to 2.8 eV. The scattering at low count rates leads to an uncertainty lower than 3% in the relative WF determination.

In Fig. 5 the results for three measurement series with the second, much brighter, LED in dc mode are shown. To avoid detector saturation at low WF, the forward current of the LED was reduced to lower the photon flux. When the count rate got too low for increasing WF, the LED current was increased from the initial value of 0.1 (black circles) to 0.6 (black squares) to 1 mA (black diamonds) and finally to the rated 10 mA (black triangles). For each current increase and series, an overlap region was chosen where the photoelectric current was measured for both, the lower and the larger current.

With this method the WF could be followed up to about 3.3 eV. After thermal heating and application of a new Cs layer, a second series was performed again at 0.6 (empty squares) and at 10 mA (empty triangles). The calibration curves of the first series could be reproduced well for the corresponding forward currents. The last measurement series (black down triangles) was performed after a weak heating of the surface to evaporate the adsorbed residual gas which left a fraction of monolayer coverage of Cs. The measured data also fit well together with the other measurements showing that the current function $I(\Phi)$ does not depend on initial conditions of the surface. It is, however, important to notice that the calibration curves are specific to our setup (e.g., surface, Cs layer, LED, optical path).

In Fig. 6 the results for the second LED driven in the ac mode are shown. Because in pulsed mode the electrons are ejected in short bursts, the saturation of the detector occurs already at 1×10^4 counts per second. At low WF the current had again to be reduced to avoid detector saturation. This was achieved with a lower bias voltage over the driving circuit. The measurements were performed at 20 (circles), 200 (squares) and 300 V (diamonds). The circuit was operating at 10 kHz for all measurements. The difference for the two higher bias voltages is marginal. With the two settings at 20 and 300 V, the WF can be followed from 2.4 eV up to 3.3 eV. A second measurement of the calibration curve $I(\Phi)$ with an other LED of the same type was made (open diamonds) at 10 kHz and 300 V. This calibration curve lies below the one for 300 V of the previous LED. If multiplied

with a factor of about 3 the two curves match reasonably well (dotted line). The experimental setup described in Sec. III had to be rebuilt before the measurement was made because of other measurements that were performed in the meantime. The mean intensity of the LED, the focusing lens system outside the vacuum chamber, the relative position of the detector and of the surface under consideration, and the detector voltage are all factors influencing I_0 in Eq. (2). Thus the difference between the two measurement series is not surprising.

V. DISCUSSION

Having established the calibration curves (Figs. 5 and 6) for a particular LED and operating conditions, one can deduce the WF of the surface simply from the photoemission current in the range from 2 eV up to 3.3 eV with a single blue LED and a detection device for electrons. The absolute accuracy is at best as good as our photoelectric measurement we use to calibrate the LED measurement. Systematic errors involved within the WF measurement with the monochromator persist in the WF determination and are not considered here. We estimate the relative reproducibility in the WF determination to ~ 0.02 eV. The promising method using a pulsed InGaN/AlGaN LED emitting in the UV range[14] showed an improvement over standard blue GaN LEDs. In the course of our measurements we found that this type of LED emits enough UV light already under nominal operating conditions in dc mode to accomplish a WF measurement in the same range. This makes the simpler method the more favorable. The photocurrent has to be measured from single counts to some pA in our setup. We made no effort to optimize the setup for quantum efficiency. If the LED would be placed in close proximity of the surface in the vacuum chamber, no photons would be lost and the measured current would increase by some orders of magnitude. The MCP based measurement in our setup saturates at 4×10^4 counts per second and for measurements in pulsed mode even at 10^4 counts per second due to bursts. This problem can simply be circumvented if the diode is driven at lower currents for lower WF or by using a detection device with a higher dynamic range (like a discrete dynode secondary electron multiplier or a pico-amperemeter).

This method to measure the WF is particularly well suited for satellite experiments like for the imaging neutral mass spectrograph LENA.[3] After an initial calibration, the WF can be measured in space simply by illuminating the conversion surface with the LED fixed in proximity and by measuring the photoelectric current. The weight and size are small, the peak power consumption is of the order of a few Watts in ac mode and a few 100 mW in dc mode. If the WF has to be measured only a few times a day, the overall power consumption is negligible.

ACKNOWLEDGMENTS

We gratefully acknowledge the free sample of the driving circuit for the pulsed LED provided to us by T. Araki, University of Tokushima. Furthermore, the authors are grateful to P. Bochsler for stimulating discussions. This work was supported by the Swiss National Science Foundation.

[1] P. Wurz, M. R. Aellig, P. Bochsler, A. G. Ghielmetti, E. G. Shelley, S. A. Fuselier, F. Herrero, M. F. Smith, and T. S. Stephen, Opt. Eng. **34**, 2365 (1995).
[2] T. Moore, D. Chornay, M. Collier, F. Herrero, J. Johnson, M. Johnson, J. Keller, J. Laudadio, J. Lobell, K. Ogilvie, P. Rozmarynowski, M. Smith, S. Fuselier, A. Ghielmetti, E. Hertzberg, D. Hamilton, R. Lundgren, P. Wilson, P. Walpole, T. Stephen, B. VanZyl, P. Wurz, and J. Quinn, Space Sci. Rev. (in press).
[3] J. Burch, *Imager for Magnetopause-to-Aurora Global Exploration (IMAGE)*, NASA MIDEX program (Southwest Research Institute, San Antonio, TX, 1995).
[4] R. Schletti, Masters thesis, University of Bern, Switzerland, 1996.
[5] M. R. Aellig, P. Wurz, R. Schletti, P. Bochsler, A. G. Ghielmetti, E. G. Shelley, S. A. Fuselier, J. M. Quinn, F. Herrero, and M. F. Smith, in *Measurement Techniques in Space Plasmas: Fields*, edited by R. F. Pfaff, J. E. Borovsky, and D. T. Young (American Geophysical Union, Washington, DC, 1998), Vol. 103, pp. 289–294.
[6] N. D. Lang, Phys. Rev. B **4**, 4234 (1971).
[7] J. N. M. van Wunnik, J. J. C. Geerlings, and J. Los, Surf. Sci. **131**, 1 (1983).
[8] J. J. C. Geerlings, P. W. van Amersfoort, L. F. T. Kwakman, E. H. A. Granneman, and J. Los, Surf. Sci. **157**, 151 (1985).
[9] P. W. van Amersfoort, J. J. C. Geerlings, L. F. T. Kwakman, A. Hershcovitch, E. H. A. Granneman, and J. Los, J. Appl. Phys. **58**, 3566 (1985).
[10] R. E. Fowler, Phys. Rev. **38**, 45 (1931).
[11] M. R. Aellig, Masters thesis, University of Bern, Switzerland, 1995.
[12] T. Fröhlich, Masters thesis, University of Bern, Switzerland, 1999.
[13] S. Nakamura, T. Mukai, and M. Senoh, J. Appl. Phys. **76**, 8189 (1994).
[14] T. Araki and H. Misawa, Rev. Sci. Instrum. **12**, 5469 (1995).